Molecules and Cells

MiR-199a/b-5p Inhibits Lymphangiogenesis by Targeting Discoidin Domain Receptor 1 in Corneal Injury

Sooeun Oh[1], Minkoo Seo[1], Jun-Sub Choi[2], Choun-Ki Joo[2,3], and Suk Kyeong Lee[1,*]

[1]Department of Medical Lifescience, [2]Catholic Institute for Visual Science, College of Medicine, The Catholic University of Korea, Seoul 06591, Korea, [3]Department of Ophthalmology and Visual Science, Seoul St. Mary's Hospital, Seoul 06591, Korea
*Correspondence: sukklee@catholic.ac.kr
http://dx.doi.org/10.14348/molcells.2018.2163
www.molcells.org

Discoidin domain receptor 1 (DDR1) is involved in tumorigenesis and angiogenesis. However, its role in lymphangiogenesis has been unknown. Here, we tested whether downregulation of DDR1 expression by miR-199a/b can suppress lymphangiogenesis. We also aimed to identify miRNA target site(s) in the 3′ untranslated region (UTR) of *DDR1*. Transfection with miR-199a/b-5p mimics reduced expression of DDR1 and tube formation in primary human dermal lymphatic endothelial cells, whereas miR-199a/b-5p inhibitors showed the opposite effects. Critically, injection of miR-199a/b-5p mimics suppressed DDR1 expression and lymphangiogenesis in a corneal alkali-burn rat model. The three well-conserved seed matched sites for miR-199a/b-5p in the *DDR1* 3′-UTR were targeted, and miRNA binding to at least two sites was required for DDR1 inhibition. Our data suggest that DDR1 promotes enhanced lymphangiogenesis during eye injury, and miR-199a/b-5p suppresses this activity by inhibiting DDR1 expression. Thus, this miRNA may be useful for the treatment of lymphangiogenesis-related eye diseases.

Keywords: corneal injuries, DDR1, endothelial cell, hsa-miR-199, lymphangiogenesis

INTRODUCTION

Lymphangiogenesis has been implicated in the rejection of corneal transplantation (Ling et al., 2008) as well as the pathophysiology of numerous eye disorders, such as choroid angiogenesis, macular edema, and eye tumors (Goyal et al., 2010; Regenfuss et al., 2008; Yang et al., 2016). For example, a C57BL/6 mouse model of dry eye syndrome demonstrated increased lymphangiogenesis and enhanced expression of lymphangiogenesis-related factors in the center of the cornea, whereas angiogenesis was not observed (Goyal et al., 2010). Lymphangiogenesis is triggered by inflammation, wound healing, keratoplasty, and tumor invasion (Bachmann et al., 2008; Flister et al., 2010; Paavonen et al., 2000), and several signal transduction pathways are involved in this process. The proteins VEGF-C and -D are strong lymphangiogenic factors (Jussila and Alitalo, 2002), and both lymphatic vessel endothelial hyaluronan receptor-1 (LYVE-1) and podoplanin are expressed specifically in lymphatic endothelial cells (Breiteneder-Geleff et al., 1999; Jackson et al., 2001).

Previously, we demonstrated that the microRNA (miRNA) hsa-miR-466 inhibits Prospero homeobox 1 (*PROX1*) expression and suppresses lymphangiogenesis in human dermal

Received 11 August, 2017; revised 2 November, 2017; accepted 10 November, 2017; published online 2 February, 2018

eISSN: 0219-1032

lymphatic endothelial primary cells (HDLECs), which are primary cells that generate lymphatic vessels (Kerjaschki et al., 2011; Nakanishi et al., 2016; Seo et al., 2015). In addition, treatment with a miR-466 mimic reduced corneal turbidity and inhibited both lymphangiogenesis and angiogenesis in a corneal alkali-burn rat model (Seo et al., 2015). These data support the potential efficacy of miRNA-based therapies for treating eye diseases involving lymphangiogenesis.

Discoidin domain receptors (DDRs) are a unique subfamily of receptor tyrosine kinases (RTKs) that interact with various collagens (Shrivastava et al., 1997). DDR1 is expressed in epithelial cells, endothelial cells, and tumor cells, whereas DDR2 is expressed mainly in mesenchymal cells (Borza and Pozzi, 2014; Heinzelmann-Schwarz et al., 2004; Johansson et al., 2005; Sakamoto et al., 2001; Song et al., 2016; Yamanaka et al., 2006). DDR1 interacts with almost all types of collagen, including fibrillar collagens I-III (Shrivastava et al., 1997; Vogel et al., 1997), and binding of DDR1 to type-specific collagens causes slow, but persistent, tyrosine autophosphorylation, which differs from the actions of other RTKs (Leitinger, 2014; Leitinger and Hohenester, 2007). Autophosphorylation of DDR1 triggered by collagen binding induces cell proliferation and tumor angiogenesis through the extracellular signal-regulated kinase (ERK) pathway (Xiao et al., 2015). It is noteworthy that lymphangiogenesis is also activated by the ERK signaling pathway (Wissmann and Detmar, 2006), suggesting that DDR1 may also be involved in lymphangiogenesis.

The miRNA miR-199a/b targets and downregulates DDR1 expression, and this activity has been found to modulate cell proliferation, migration, invasion, and tumor progression in breast cancer, colorectal cancer, hepatocellular carcinoma, and acute myeloid leukemia (Fau et al., 2012; Hu et al., 2014; Mata et al., 2016; Shen et al., 2010). Additionally, miR-199a/b can regulate angiogenesis by targeting hypoxia-inducible factor-1 alpha (HIF-1α), podocalyxin (PODXL), and DDR1 (Das et al., 2006; Fau et al., 2012; Xiao et al., 2015). However, the role of this miRNA in lymphangiogenesis is unclear, and the exact target sites for miR-199a/b binding in the *DDR1* mRNA are unknown.

In this study, we investigated the effects of miR-199a/b on DDR1 expression and lymphatic endothelial cell tube formation by HDLECs in culture. We further explored the role of these factors on corneal lymphangiogenesis *in vivo* using an alkali-burn rat model. Lastly, we identified the miR-199a/b target sites in the 3′ untranslated region (UTR) of *DDR1* and demonstrated their role in DDR1 regulation.

MATERIALS AND METHODS

Cells

Primary HDLECs from juvenile foreskin were purchased from PromoCell (Cat No. c-12216; Germany) and cultured in MV2 medium containing 10 ng/ml bFGF, 5 ng/ml EGF, and 20 ng/ml IGF-1 (PromoCell). HEK293T human embryonic kidney cells were cultured in Dulbecco's Modified Eagle's Medium (Gibco BRL, USA) supplemented with 10% fetal bovine serum and antibiotics (100 U/ml penicillin and 100 μg/ml streptomycin; Gibco BRL). All cells were maintained at 37℃ in the presence of 5% CO_2.

miRNA mimics, siRNA, and miRNA inhibitors

The miRNA mimics, DDR1 siRNA (siDDR1), and scrambled control miRNA used as a negative control were purchased from Genolution Pharmaceuticals (South Korea). Sequences were as follows: 5′-CCCAGUGUUCAGACUACCUGUUC-3′ (miR-199a-5p mimic), 5′-CGGTGUGUUCAGACUACCUGUUC-3′ (miR-199a-5p mimic mutant; miR-199a-5pm), 5′-CCCAGUGUUUAGACUAUCUGUUC-3′ (miR-199b-5p mimic), 5′-CCCAGUGUUUAGACUAUCUGUUC-3′ (miR-199b-5p mimic mutant; miR-199b-5pm), 5′-UCUGGAGGGAUGGACUCCUGUCUUAUU-3′ (siDDR1), 5′-UUUUAACUCAGUAUUUUUA-3′ (scrambled control). The miRNA inhibitors for miR-199a/b-5p and a negative control inhibitor were purchased from Exiqon (Denmark). Sequences were as follows: 5′-TAACACGTCTATACGCCCA-3′ (negative control inhibitor), 5′-AACAGGTAGTCTGAACACT-3′ (miR-199a-5p inhibitor), 5′-ACAGATAGTCTAAACACT-3′ (miR-199b-5p inhibitor).

Luciferase reporter plasmid construction and site-directed mutagenesis

The 3′-UTR of *DDR1* was amplified from the genomic DNA of Akata cells and cloned between the Renilla luciferase coding sequence and the poly(A) site of the psiCHECK-2 plasmid (Promega, USA) using *Xho*I/*Not*I sites to produce psiC-DDR1. The primers for amplification of the *DDR1* 3′-UTR were 5′-TCTAGGCGATCGCTCGAGCCTCAGGGAGCGATCCAG-3′ and 5′-TTATTGCGGCCAGCGGCCGCCTGCCTAGTGCAGGGGATTA-3′. Mutations were introduced into the putative seed match sequences of psiC-DDR1 using the EZchange Site-Directed Mutagenesis Kit (Enzynomics, Korea). The primer sequences were psiC-DDR1_m1: 5′-TCTGTCTATCCTATATTTCTCCCCACCCT-3′ and 5′-CCACATGGCCCATTGGAGCAC-3′; psiC-DDR1_m2: 5′-TCTGTGTGACAGGGAGAGAGAAGC-3′ and 5′-CCACCCCATGGCTGAGAATCT-3′; psiC-DDR1_m3: 5′-TCTGTTTCAGGTGATGGAGGAGGAA-3′ and 5′-CCACCTGGGGGTAGCCCCGC-3′.

Luciferase reporter assay

To test whether the miRNAs directly target the 3′-UTR of *DDR1*, a luciferase reporter assay was performed. HEK293T human embryonic kidney cells, which are frequently used for luciferase reporter assays (Kim et al., 2015; Lossner et al., 2011; Xu et al., 2012) and HDLECs were seeded in 96-well plates (5×10^3 cells/well). After 24 h, cells were co-transfected with 10 nM of each miRNA mimic and 20 ng psiC-DDR1 or a mutant reporter vector (psiC-DDR1_m1, psiC-DDR1_m2, psiC-DDR1_m3, psiC-DDR1_m1m2, psiC-DDR1_m2m3, psiC-DDR1_m1m3, or psiC-DDR1_m1m2m3). Luciferase activity was measured at 48 h post-transfection using the Dual-Glo™ Luciferase Assay System (Promega). Renilla luciferase activity was normalized using the firefly luciferase activity for each sample.

Transfection of HDLECs

Cells were seeded for 24 h prior to transfection in 60 or 100 mm diameter dishes containing 5 or 10 ml of culture medium, respectively. Transfection was performed with 20 nM of

each miRNA mimic, siRNA, or miRNA inhibitor using Lipofectamine™ 2000 (Invitrogen), according to the manufacturer's protocol. Cells were harvested for RNA and protein extraction 48 h post-transfection.

Quantitative reverse transcription-polymerase chain reaction (qRT-PCR)

HDLECs were harvested, and total RNA was extracted using RNAiso Plus (Takara, Japan), according to the manufacturer's instructions. Complementary DNA (cDNA) was synthesized using 1 μg total RNA, oligo(dT) (Macrogen, South Korea), and M-MLV reverse transcriptase (Invitrogen). For miRNA detection, cDNA was synthesized using mir-X™ miRNA First-Strand Synthesis Kit (Takara), according to the manufacturer's instructions. Real-time PCR for *DDR1* or miR-199a/b-5p was carried out using the TOPreal™ qPCR 2X PreMIX (*SYBR Green with low ROX*; Enzynomics, Daejeon, Korea) with the CFX96 Real-Time PCR System (Bio-Rad, USA). Primer sequences were as follows: *DDR1*, 5′-AATCGCAGACTTTGGCATGAG-3′ and 5′-CGTGAACTTCCCCATGAGGAT-3′; glyceraldehyde phosphate dehydrogenase (*GAPDH*), 5′-ATGGGGAAGGTGAAGGTCG-3′ and 5′-GGGGTCATTGATGGCAACAATA-3; miR-199a-5p, 5′-CCCAGTGTTCAGACTACCTGTTC-3′; miR-199b-5p, 5′-CCCAGTGTTTAGACTATCTGTTC-3′. For U6 amplification, the primers included in the mir-X™ miRNA First-Strand Synthesis Kit were used. PCR conditions were as follows: 95℃ for 10 min, followed by 40 cycles at 95℃ for 20 s, 60℃ for 30 s, and 72℃ for 30 s for *DDR1/GAPDH* detection, and 95℃ for 10 min, followed by 40 cycles at 95℃ for 5 s and 60℃ for 20 s for miR-199/U6 detection. To confirm specific amplification of PCR products, dissociation curves were checked routinely. PCR products were ramped up from 55℃ to 95℃ at a heating rate of 0.1℃/s, and fluorescence was measured continuously. Relative gene expression was calculated according to the comparative Ct method using *GAPDH* (for *DDR1*) or U6 (for miRNAs) as an internal standard.

Tube formation assay

Endothelial cells were plated on a reconstituted basement membrane matrix, which promotes the formation of capillary-like tubules, as well as rapid attachment and alignment of cells (Arnaoutova et al., 2009). This endothelial cell-specific process is rapid and quantifiable; therefore, tube formation has been used to study angiogenic and anti-angiogenic factors, to investigate mechanisms of angiogenesis, and to define endothelial cell populations. Here, we utilized tube formation experiments to assess the effect of miRNAs on lymphangiogenesis in HDLECs, using an In Vitro Angiogenesis Assay Kit (Millipore), according to the manufacturer's protocol. Briefly, eight-well chamber slides were coated with cold liquid ECMatrix (130 μl/well) and incubated at 37℃ in a humidified 5% CO_2 incubator for 1 h to promote solidification. Cells transfected with miRNAs (10^5 cells/well) were then seeded into these polymerized ECMatrix-coated chamber slides and incubated with conditioned medium at 37℃ for 4-6 h. To detect tube formation more clearly, cells were stained in a medium containing 5 μM calcein^{AM} for 1 h. Formation of tube-like structures was observed by fluorescence microscopy and quantified by counting the number of tubes formed in three randomly chosen fields using ImageJ software (National Institutes of Health [NIH], USA).

Experimental corneal alkali-burn animal model

Male Sprague-Dawley rats (body weight approximately 250-300 g, $n = 5$ for each group) were utilized for this study. All the animals were treated in accordance with the guidelines of the Association for Research in Vision and Ophthalmology Statement for the Use of Animals in Ophthalmic and Vision Research. The study protocol was approved by the Committee for Animal Research, Catholic University of Medicine. Rats were deeply anesthetized via intraperitoneal injection of 50 mg/kg tiletamine plus zolazepam (Zoletil; Virbac, France) and 15 mg/kg xylazine hydrochloride (Rompun; Bayer, Leuverkeusen, Germany). Alkali injuries to the eyes were induced by a 10-s exposure of the central cornea to a 4-mm diameter disk of filter paper soaked in 0.5 N NaOH, followed by rinsing with 1 ml sterile saline. To avoid corneal infection, one drop of 0.5% levofloxacin (Cravit; Sante, Japan) was dispensed onto the ocular surface immediately after alkali-burn injury. Animals were then randomly assigned to three treatment groups: scrambled control, miR-199a-5p, and miR-199b-5p ($n = 5$ for each). All mice were treated with a single subconjunctival injection of 20 nM miRNA (20 μl) immediately following alkali-burn injury.

To test the effect of DDR1 inhibition for lymphangiogenesis, mice were randomly allocated to seven groups (n = 3). One group was used as a normal control without treatment. For the other six groups, alkali injuries to the eyes were induced and treated with indicated miRNA as described above. A DDR1 inhibitor 7rh (Sigma-Aldrich, USA) was dissolved in DMSO to make 2.5 mg/ml stock solution and 1/10 diluted in PBS before use. Three groups of mice were co-injected subconjunctivally with a DDR1 inhibitor 7rh together with miRNA immediately following alkali-burn injury. One mouse of each group was used for LYVE-1 immunostaining of cornea. Corneas were isolated from the other two mice of each group for Western blot analysis.

Western blot analysis

HDLECs were harvested and corneal tissues were ground using Dounce tissue grinder set (Sigma-Aldrich) before adding radioimmunoprecipitation assay (RIPA) buffer. Samples were mixed with 5X loading buffer (Fermentas, USA), heated at 92℃ for 5 min, separated by 10% sodium dodecyl sulfate-polyacrylamide gel electrophoresis (SDS-PAGE), and transferred to polyvinylidene fluoride (PVDF) membranes (Millipore, USA). Membranes were incubated overnight at 4℃ with rabbit polyclonal antibodies to DDR1 (1:500; Santa Cruz Biotechnology, USA), lymphatic vessel endothelial hyaluronan receptor-1 (LYVE-1) (1:1000; Novus biologics, USA), podocalyxin (PODXL) (1:1000; Santa Cruz Biotechnology), or hypoxia-inducible factor-1 alpha (HIF1α) (1:1000; Novus biologics). After washing with 0.5X tris-buffered saline with tween 20 (TBST) for 1 h, blots were incubated for 1 h at room temperature with horseradish peroxidase-conjugated anti-rabbit secondary antibody (1:5000; Santa Cruz Biotech-

nology), and protein bands were visualized using an enhanced chemiluminescence detection system (Amersham Biosciences, USA). A β-actin antibody (1:1000; Cell Signaling Technology, USA) was used to confirm comparable loading. The density of each protein band was determined using Fujifilm Multi Gauge version 3.0 software.

Immunostaining

Formalin-fixed corneas were embedded in paraffin, and 4-μm sections were prepared for examination. To detect DDR1, corneal sections were incubated with anti-DDR1 antibody (dilution, 1:500; Santa Cruz Biotechnology) for 1 h and washed three times with phosphate buffered saline (PBS). Corneal sections were then treated with a Texas Red-conjugated secondary antibody (Abcam, USA) and stained with Hoechst solution to visualize the nuclei prior to examination by fluorescence microscopy at 100X magnification. To assess lymphangiogenesis, a corneal flat mount was utilized for lymphatic vessel endothelial hyaluronan receptor-1 (LYVE-1) immunostaining. For this assay, whole corneas were isolated from the eye and incubated with anti-mouse LYVE-1 antibody (1:500; Abcam) for 16 h at 4℃. After three washes with PBS for 15 min, corneas were stained with a Texas Red-conjugated secondary antibody (Abcam). The stained areas were calculated by ImageJ software version 4.01 (NIH, USA), and values were expressed as ratios to measurements obtained from animals treated with the scrambled control.

Statistical analysis

Data were analyzed using a Student's *t*-test. Curve fit and analysis were performed using GraphPad Prism software (GraphPad Software, USA). *P*-values < 0.05 were considered statistically significant. All results are expressed as mean ± standard deviation (SD).

RESULTS

Effect of miRNA mimics on the expression of DDR1 mRNA and protein

To determine whether miR-199a/b-5p modulates the expression of DDR1 in lymphatic endothelial cells, HDLECs were transfected with the miRNA mimics, miR-199a-5p and miR-199b-5p, as well as the scrambled control. Total RNA was then prepared from cells harvested at 48 h post-transfection, and *DDR1* expression was determined by qRT-PCR. Our data demonstrate that levels of *DDR1* mRNA were decreased by approximately 50-60% following transfection with either miR-199 mimic compared to the scrambled control (Fig. 1B). Western blot analysis also showed that DDR1 protein expression decreased by approximately 60-70% following transfection with miR-199a/b-5p mimics compared to the control (Fig. 1C). As an additional control, we transfected HDLECs with mutant versions of the miRNA mimics (miR-199a-5pm and miR-199b-5pm), which are predicted to be inactive. As expected, expression of DDR1 protein was not considerably affected by these mutant miRNAs (Figs. 1A and 1C).

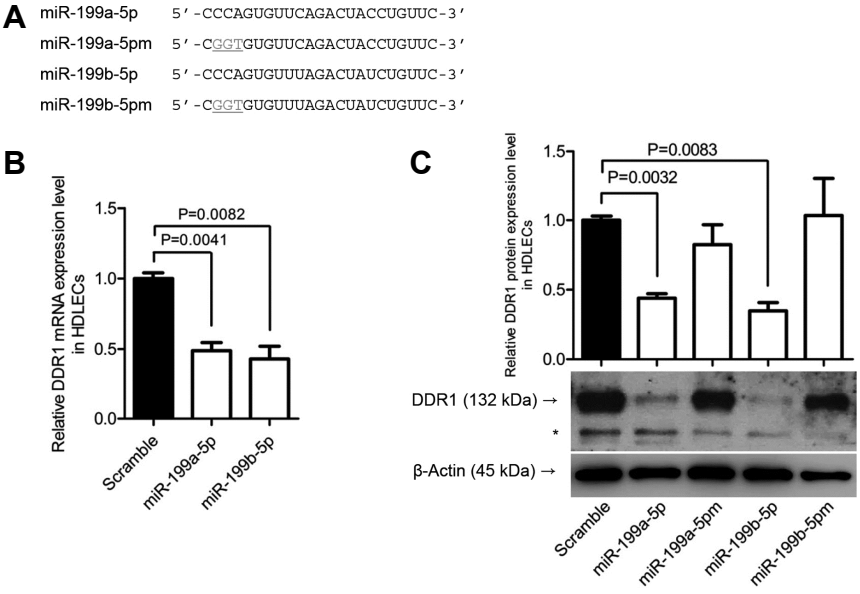

Fig. 1. Effects of miR-199a/b-5p mimics on expression of DDR1 mRNA and protein. (A) Sequence of miR-199a/b-5p and the mutant forms of miR-199a/b-5p (miR-199a/b-5pm); mutants have nucleotide substitutions at two to four sites within the miRNA. (B) Reduction in *DDR1* mRNA levels by miR-199a/b-5p. HDLECs were transfected with 20 nM miR-199a/b-5p mimics or the scrambled control, and levels of DDR1 mRNA were measured by qRT-PCR. Relative gene expression was calculated according to the comparative Ct method, using *GAPDH* as an internal control ($n = 3$). Error bars indicate standard deviation (SD). (C) Effects of miR-199a/b-5p on DDR1 protein expression. HDLECs were transfected with 20 nM miR-199a/b-5p mimics or the scrambled control. To confirm the sequence-specific function of miR-199a/b-5p, miR-199a/b-5p mutants (miR-199a/b-5pm) were also transfected. Cell lysates were examined by Western blot analysis with an anti-DDR1 polyclonal antibody (1:500) at 48 h post-transfection; an anti-β-actin antibody (1:1000) was used to normalize protein loading. Three sets of independent experiments were performed, and representative results are shown in the lower panel; asterisk (*) indicates nonspecific band. The density of each protein band was quantified using Fujifilm Multi Gauge software version 3.0 and expressed as a ratio to the density of the band from the scrambled control. Upper panel shows mean ± SD values of the three independent experiments.

Elucidation of miR-199a/b-5p target sites in the 3′-UTR of *DDR1* mRNA

To determine whether miR-199a/b-5p directly targets the 3′-UTR of human *DDR1* mRNA, we co-transfected HEK293T cells or HDLECs with each miRNA mimic and the psiC-DDR1 luciferase reporter vector. Mutant forms of miR-199a-5p and miR-199b-5p (miR-199a-5pm and miR-199b-5pm) were also used to confirm the sequence-specific function of each miRNA mimic. We found that the miR-199a/b-5p mimics significantly reduced luciferase activity from psiC-DDR1, as compared to the scrambled control in HEK293T (Fig. 2A) and HDLECs (Fig. 2B). In contrast, psiC-DDR1 luciferase activity was not affected by either of the mutant miRNAs in both cells (Figs. 2A and 2B). The TargetScan program (http://www.targetscan.org) predicts that miR-199a/b-5p has three well-conserved 8mer seed matches with the human *DDR1* 3′-UTR. Thus, we utilized site-directed mutagenesis to assess which sites are directly targeted by miR-199a/b-5p. Single, double, or triple mutations were introduced in the three well-conserved seed match sequences to produce reporter vectors with seven mutant forms of the 3′-UTR (psiC-DDR1_m1, psiC-DDR1_m2, psiC-DDR1_m3, psiC-DDR1_m1m2, psiC-DDR1_m2m3, psiC-DDR1_m1m3, and psiC-DDR1_m1m2m3; Figs. 2C and 2D). Each of these vectors was co-transfected into HEK293T cells with miR-199a/b-5p or the scrambled control, and luciferase activity was measured. We found that luciferase activity from the single mutant vectors (psiC-DDR1 m1, psiC-DDR1 m2, and psiC-DDR1 m3) was partially reduced when the cells were co-transfected with miR-199a/b-5p mimics (Figs. 2E and 2F).

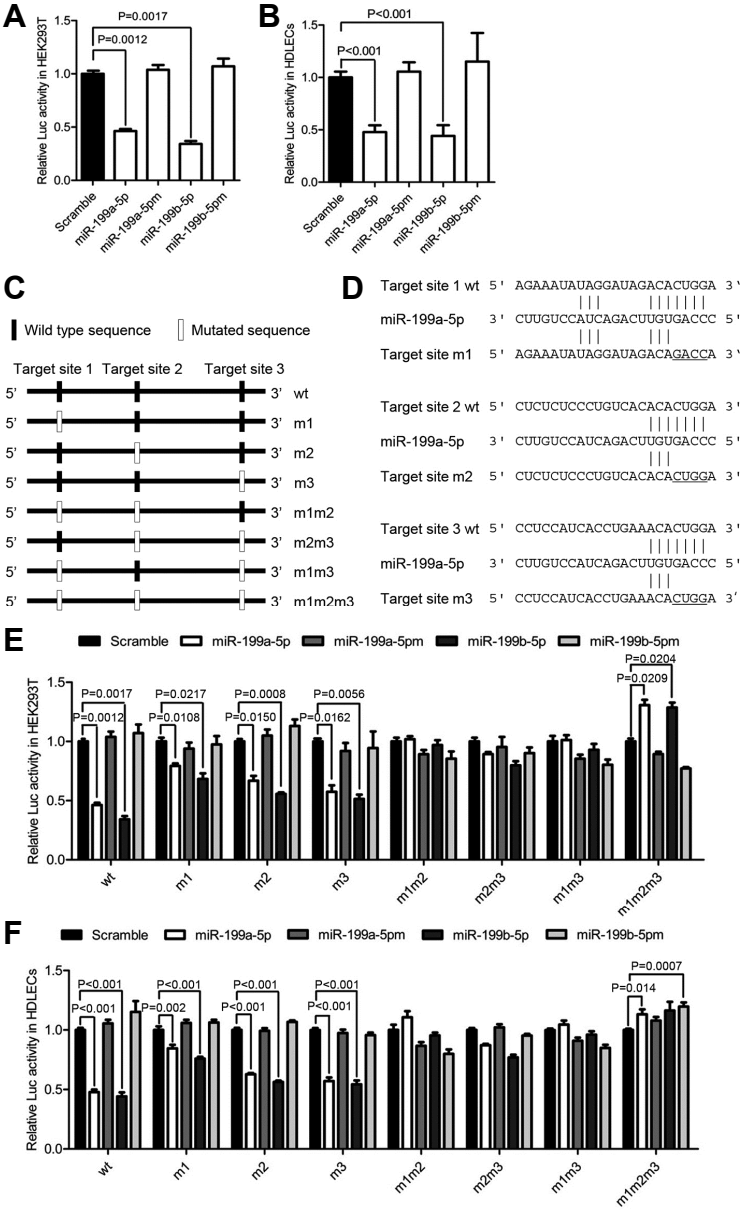

Fig. 2. Luciferase reporter assay to identify miR-199a/b-5p target sites in the *DDR1* 3′-UTR. (A, B) Luciferase reporter assay testing the effect of miR-199a/b-5p on DDR1. A reporter construct containing (psiC-DDR1) the *DDR1* 3′-UTR and the Renilla luciferase gene was co-transfected into HEK293T cells or HDLECs with the miR-199a/b-5p mimics. To confirm the sequence-specific function of miR-199a/b-5p, the miR-199a/b-5pm (mutant miRNA), which have nucleotide substitutions at two to four sites of miR-199a/b-5p, were also used. Error bars indicate SD (n = 3). (C) Illustration showing the location of possible seed matched sites for miR-199a/b-5p in the *DDR1* 3′-UTR. Site-directed mutagenesis was performed to produce all possible mutant forms of the *DDR1* 3′-UTR seed match sequences. Mutation signatures are as follows: m1 (psiC-DDR1_m1), m2 (psiC-DDR1_m2), m3 (psiC-DDR1_m3), m1m2 (psiC-DDR1_m1m2), m2m3 (psiC-DDR1_m2m3), m1m3 (psiC-DDR1_m1m3), and m1m2m3 (psiC-DDR1_m1m2m3). (D) Seed matches between miR-199a/b-5p and the wild-type (wt) or mutated (m1, m2, or m3) target sites in the 3′-UTR of *DDR1*. Bottom bars indicate mutated nucleotides in m1, m2, and m3 (E, F). Luciferase reporter assay testing the target sites of miR-199a/b-5p on the 3′-UTR of DDR1. HEK293T cells or HDLECs were co-transfected with miR-199a/b-5p and luciferase reporter vectors containing the wt or mutated 3′-UTR of *DDR1*. The scrambled control and miR-199a/b-5pm (mutant miRNA) were used to confirm sequence-specific binding between miR-199a/b-5p and the *DDR1* 3′-UTR. Luciferase activity was normalized using firefly luciferase activity and is expressed as the ratio to the activity in scrambled control-transfected cells. Error bars indicate SD (n = 3).

However, activity from each double mutant vector (psiC-DDR1_m1m2, psiC-DDR1_m2m3, and psiC-DDR1_m1m3) was not significantly affected in the cells co-transfected with the miR-199a/b-5p mimics (Figs. 2E and 2F). Unexpectedly, luciferase activity from the triple mutant vector, psiC-DDR1_m1m2m3, was increased in cells co-transfected with the miR-199a/b-5p mimic or miR-199-5pm as compared to scrambled control (Figs. 2E and 2F). The reason for this is not clear, and we did not pursue this unexpected observation any further. As expected, luciferase activity from the wild-type or mutated *DDR1* 3'-UTR reporter vectors was not affected by co-transfection with the scrambled control, a mutant form of miR-199a-5p (miR-199a-5pm), or a mutant form of miR-199b-5p (miR-199b-5pm) (Figs. 2E and 2F).

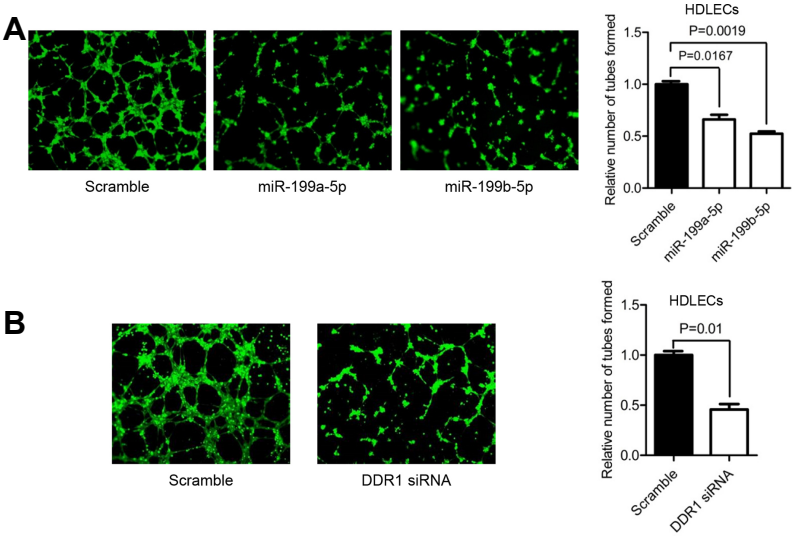

Fig. 3. Effect of miR-199a/b-5p mimics on HDLEC tube formation. HDLECs were transfected with 20 nM miR-199a/b-5p mimics (A) or siRNA targeting DDR1 (siDDR1) (B). Scrambled control siRNAs were used for comparison. After 48 h, cells (10^5 cells/well) were plated in an ECMatrix-coated eight-well chamber in MV2 medium, containing 10 ng/ml bFGF, 5 ng/ml EGF, and 20 ng/ml IGF-1. To detect the tube formation more clearly, the cells were stained in a media containing 5 μM calcein AM for 1 h. Capillary-like structures within the Matrigel layer formed by HDLECs were photographed after 4-6 h at 50X magnification. Three independent experiments were performed for each condition and representative results are shown in the left panels. Tube formation was quantified using ImageJ software, and the mean ± SD values are plotted in the right panels ($n = 3$).

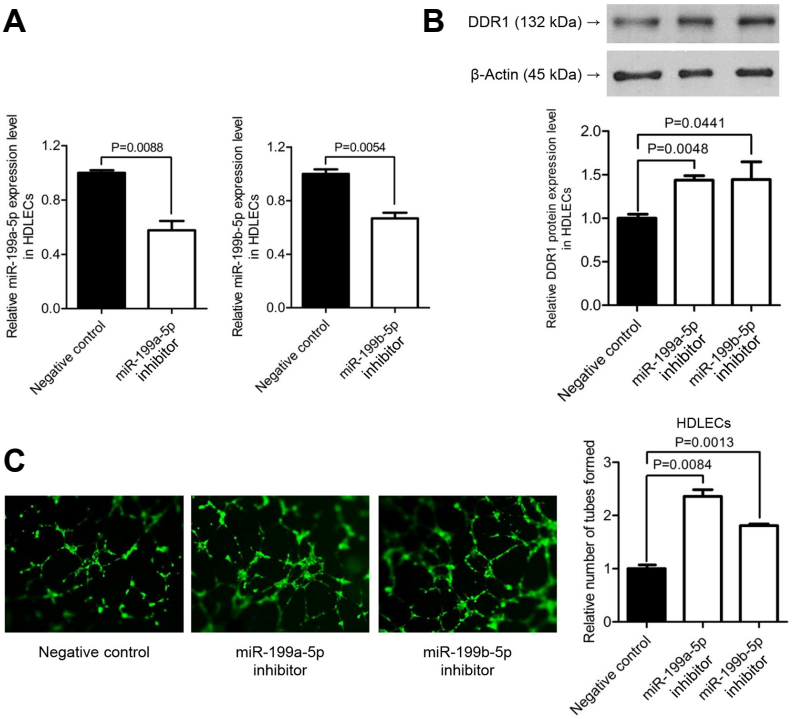

Fig. 4. Effect of miR-199a/b-5p inhibitors on HDLEC tube formation. (A) Effect of miRNA inhibitors on the level of miR-199a/b-5p. HDLECs were transfected with 20 nM miR-199a/b-5p inhibitors or the negative control inhibitor. After 48 h, cells were harvested for qRT-PCR analysis; three independent experiments were performed, and relative miR-199a/b-5p expression was calculated according to the comparative Ct method, using U6 as an internal control ($n = 3$). Error bars indicate SD. (B) Western blot analysis to detect DDR1 expression 48 h after transfection with miR-199a/b-5p inhibitors. Three sets of independent experiments were performed and representative results are shown (upper panel). Anti-β-actin antibody (1:1000) was used to confirm comparable loading. Band densities were quantified using Fujifilm Multi Gauge software version 3.0, and relative DDR1 expression levels are plotted (lower panel). Error bars indicate SD ($n = 3$). (C) At 48 h post-transfection, cells (10^5 cells/well) were plated in an ECMatrix-coated eight-well chamber in MV2 medium, containing 10 ng/ml bFGF, 5 ng/ml EGF, and 20 ng/ml IGF-1. To detect the tube formation more clearly, the cells were stained in a media containing 5 μM calcein AM for 1 h. Capillary-like structures within the Matrigel layer formed by HDLECs were photographed after 4-6 h at 50x magnification. Three independent experiments were performed for each setting and representative results are shown at the left panels. Tube formation was quantified using ImageJ software, and the mean +/- SD values are plotted on the right panels ($n = 3$).

These results demonstrate that miR-199a/b-5p specifically targets all three of the well-conserved target sites, and if any two of these sites are mutated, the efficiency of miR-199a/b-5p targeting was significantly reduced.

Effect of miR-199a/b-5p or the inhibitors on HDLECs tube formation

We used an *in vitro* tube formation assay to determine whether miR-199a/b-5p has anti-lymphangiogenic effects. HDLECs transfected with miR-199a/b-5p mimics or the scrambled control were cultured for 48 h and then transferred to Matrigel-coated 8-well glass slides. The extent of tube formation was assessed after 2-6 h. We observed a 30-50% less tube formation in HDLECs when transfected with miR-199a/b-5p mimics than when transfected with the scrambled control (Fig. 3A). Notably, tube formation was also decreased by approximately 60% in HDLECs transfected with siDDR1 compared to the control cells (Fig. 3B).

To assess whether endogenous miR-199a/b-5p can regulate the expression of DDR1 in HDLECs, we utilized miR-199a/b-5p inhibitors. HDLEC cells were transfected with the inhibitors or a control inhibitor. qRT-PCR performed at 48 h post-transfection revealed that levels of miR-199a/b-5p were reduced by about 40-50% by transfection with each inhibitor compared to the control inhibitor (Fig. 4A). Total protein was also prepared at 48 h post-transfection. Western blot analyses demonstrated that DDR1 protein levels were increased by 40% in HDLECs transfected with the miR-199a/b-5p inhibitors compared to cells transfected with the control inhibitor (Fig. 4B). We then assessed the tube-forming ability of cells transfected with miR-199a/b-5p inhibitor. When HDLECs transfected with the miR-199a/b-5p inhibitor for 48 h were cultured on Matrigel-coated 8-well glass slides, tube formation was significantly higher than in the control cells (Fig. 4C).

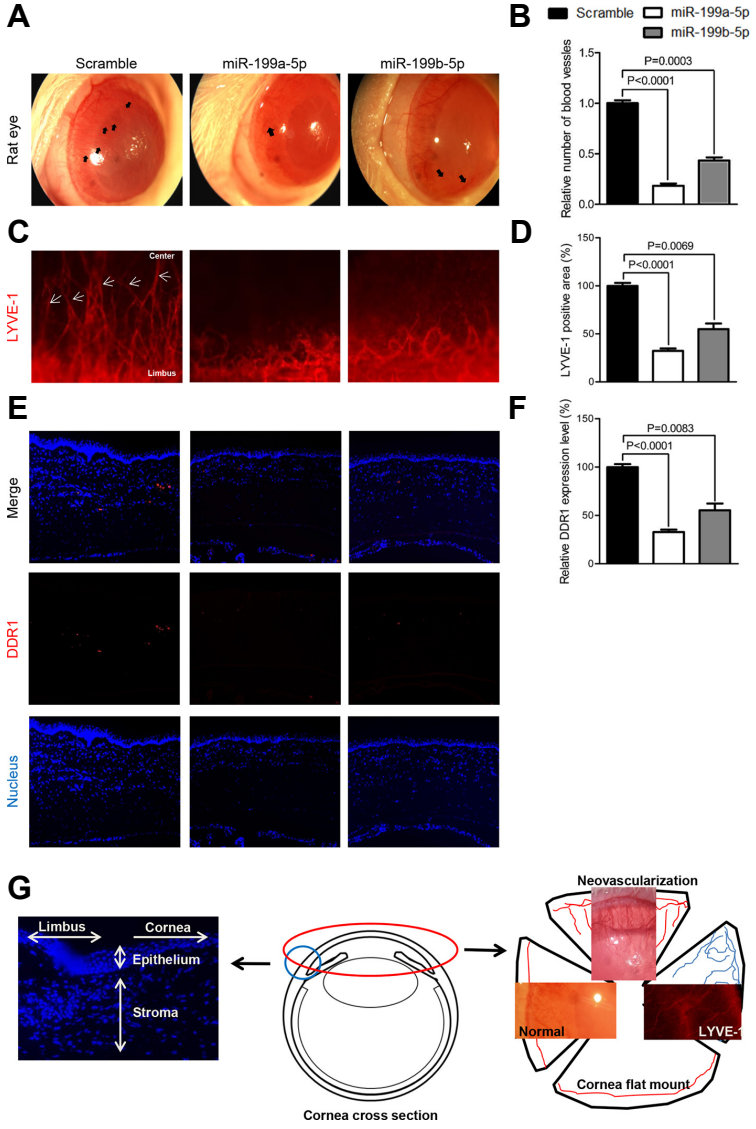

Fig. 5. Inhibition of corneal lymphangiogenesis and DDR1 expression by miR-199a/b-5p in a corneal injury animal model. Corneas of Sprague-Dawley rats were subjected to alkali burns with NaOH, and animals were treated with miR-199a/b-5p mimics or the scrambled control by subconjunctival injection on the day of injury ($n = 3$ for each treatment group). (A) Representative photographs of corneas taken one week after treatment. Corneal neovascularization of the whole rat eye was observed by light microscopy. Arrows in each panel show blood vessels formed on cornea. (B) Levels of angiogenesis were quantified for each group using ImageJ software and expressed as a ratio to the level of angiogenesis in the scrambled control group ($n = 5$). (C) Lymphatic vessel formation in the cornea. Whole corneas were flat-mounted, as shown in (G), and stained with the LYVE-1 antibody. Red stain indicates areas positive for LYVE-1, a marker of lymphatic vessels. (D) Lymphatic vessel formation was assessed in all treatment groups using ImageJ software by quantifying LYVE-1 positive areas ($n = 5$). Values are expressed as ratios to the scrambled control group. (E) DDR1 expression in the cornea. Formalin-fixed corneas from each treatment group were embedded in paraffin; these were cut into 4 μm sections and stained with anti-DDR1 antibody. Red stain represents DDR1, and blue stain indicates nuclei stained with DAPI. Similar results were obtained in two independent experiments, and one representative set is shown. (F) DDR1 expression level was assessed in all treatment groups using ImageJ software by quantifying DDR1 positive areas ($n = 5$). Original magnification, (A) 10x, (C, E) 100x. (G) Right panel shows how the corneal flat mounts were prepared for LYVE-1 staining. Neovascularization in alkali-burned cornea is also shown in contrast to clear normal cornea. Left panel shows the histological location for the paraffin sections used for DDR1 immunofluorescence assay.

Effect of miR-199a/b-5p on lymphangiogenesis in a corneal alkali-burn animal model

To confirm the effects of miR-199a/b-5p on corneal lymphangiogenesis and DDR1 expression *in vivo,* we used an experimental animal model for corneal injury. Following introduction of alkali burns in rat corneas, miR-199a/b-5p mimics or scrambled control RNA were injected once subconjunctivally, and the effects were assessed a week later. We observed severe angiogenesis in corneas subjected to alkali burn as compared to the normal cornea (Figs. 5A and 5G). Critically, the number of blood vessels formed in miR-199a/b-5p mimic-treated eyes was approximately 50-80% less than that in scrambled control-injected eyes (Figs. 5A and 5B).

To determine the effect of miR-199a/b-5p on lymphangiogenesis in the cornea, lymphatic vessels in flat-mounted corneas (illustrated in Fig. 5G) were stained with an anti-LYVE-1 antibody (Fig. 5C). We found that the LYVE-1-positive area, which indicates the region containing lymphatic vessels, was about 50-70% smaller in miR-199a/b-5p mimic-treated corneas than in scrambled control-injected corneas (Fig. 5D). DDR1 expression was then assessed in paraffin-embedded corneal sections (Fig. 5G) by immunohistofluorescence staining with an anti-DDR1 antibody. Our data demonstrate that DDR1 expression, similar to what was observed for LYVE-1, was induced at limbus and epithelium following alkali burn (Figs. 5E and 5G). DDR1 expression in corneal tissues from miR-199a/b-5p mimic-treated eyes was clearly decreased over 50% compared to scrambled control-injected eyes (Figs. 5E and 5F). However, LYVE-1 but not DDR1 was not stained at the center of corneas (Fig. 5C).

To test the effect of DDR1 inhibition on lymphangiogenesis, we used a DDR1 inhibitor 7rh (Sigma-Aldrich, USA) known to reduce DDR1 expression and phosphorylation (Lu et al., 2016). Cornea-injured rats were co-treated with DDR1 inhibitor 7rh with scrambled control or miR-199a/b-5p mimic. LYVE-1 immunostaining showed that 7rh treatment drastically suppressed lymphangiogenesis compared to the corneas untreated with 7rh (Supplementary Fig. S1A). Western blot analyses showed that a 7rh treatment effectively reduced DDR1 and LVYE-1 expression compared to the corneas untreated with 7rh (Supplementary Figs. S1B-S1D). LYVE-1 expression was further reduced when the cells were co-treated with 7rh and miR-199a/b-5p (Supplementary Figs. S1B and S1D). As expected, miR-199a/b-5p downregulated PODXL (Supplementary Figs. S1B and S1E), but 7rh did not affect PODXL expression (Supplementary Figs. S1B and S1E). Nevertheless, LYVE-1 was significantly downregulated after 7rh treatment (Supplementary Figs. S1B and S1D). HIF1α was undetected in cornea samples by Western blot (data not shown).

DISCUSSION

Previous reports have suggested that miR-199-5p modulates DDR1 expression in some tumor cells (Hu et al., 2014; Mata et al., 2016). However, the specific target site(s) for miR-199a/b-5p in the 3′-UTR of the *DDR1* gene had not been identified. Furthermore, the role of DDR1 in lymphangiogenesis was unclear. In this study, we found that miR-199a/b-5p directly targeted three sites on the 3′-UTR of *DDR1* and reduced DDR1 expression at both the mRNA and protein levels in HDLEC cells. In addition, miR-199a/b-5p suppressed tube formation of lymphatic endothelial cells in culture, seemingly by its effect on DDR1 expression. Critically, we found that *in vivo* injection of a miR-199a/b-5p mimic not only suppressed DDR1 expression, but also inhibited lymphangiogenesis in a corneal alkali-burn rat model.

The TargetScan program identified three well-conserved 8mer seed match sites for miR-199a/b-5p in the 3′-UTR of *DDR1*. When a point mutation was introduced into each of the three sites, the effect of miR-199a/b-5p on DDR1 expression was partially reduced, suggesting that all three sites are genuine targets of these miRNAs. In addition, when any two of the three seed matched sites were mutated simultaneously, the effect of miR-199a/b-5p on the expression of DDR1 disappeared completely. These results suggest that occupation of just one target site by miR-199a/b-5p is not sufficient, and that miR-199a/b-5p must bind to at least two of the three sites to suppress DDR1 expression. Considering miRNAs are generally involved in fine tuning gene expression (Ying et al., 2006), we observed significant reduction in *DDR1* expression (about 50%) by miR-199a/b-5p. This strong effect on *DDR1* may be due to the presence of multiple target sites for miR-199a/b-5p in the 3′-UTR of this gene (Bartel, 2009).

The increased DDR1 expression and enhanced tube formation following miR-199a/b-5p inhibitor treatment in HDLECs support the theory that endogenous levels of miR-199a/b-5p in these lymphatic endothelial cells are sufficient to affect DDR1 expression. These results further suggest that miR-199a/b-5p plays an important physiological role in lymphangiogenesis by inhibiting DDR1 expression.

A number of previous studies have shown that lymphangiogenesis, as well as angiogenesis, are induced in an alkali-burn injury model (Ling et al., 2009; Zhu et al., 2015). We therefore used a rat corneal alkali-burn model for this study. A single subconjunctival injection of miR-199a/b-5p mimic into corneas after alkali injury efficiently suppressed DDR1 expression and reduced corneal lymphangiogenesis.

A DDR1 inhibitor 7rh treatment not only effectively reduced DDR1 and LVYE-1 expression but also suppressed lymphangiogenesis. These results support that miR-199a/b-5p inhibited lymphangiogenesis at least partially by targeting DDR1 expression. As miR-199a/b-5p also targets PODXL and HIF1α, we wanted to test whether they are also responsible for suppressed lymphangiogenesis cause by miR-199a/b-5p. HIF1α was undetectable in cornea samples by Western blot under our experimental conditions (data not shown). PODXL was expressed at high level in normal cornea. PODXL expression was unaffected by alkali burn or 7rh treatment, but down regulated by miR-199a/b-5p. Thus, HIF1α and PODXL seem to have little role in cornea lymphangiogenesis following alkali injury.

Similar to the results shown in this study, we and other investigators have previously reported that corneal lymphangiogenesis is also significantly downregulated by a single injection of miRNAs targeting other protein species (Grimaldo et

al., 2015; Seo et al., 2015). These observations may be explained by the fact that the cornea is an isolated tissue, and/or transient modulation of miRNA function may be sufficient for long-term suppression of corneal lymphangiogenesis.

Our results demonstrate that miR-199a/b-5p directly targets the 3′-UTR of *DDR1* and downregulates the expression of this gene, resulting in the inhibition of lymphangiogenesis both in cultured human lymphatic endothelial cells and a corneal alkali-burn rat model. Our results indicate that DDR1 downregulation by miR-199a/b-5p may be therapeutically useful for treating corneal lymphangiogenesis, and DDR1 itself provides a potential target for the development of improved therapeutics for lymphangiogenic eye diseases. MiRNAs have multiple targets and modulate cellular functions, while siRNAs target and downregulate a specific gene (Lam et al., 2015). Thus, miR-199a/b-5p might target a variety of lymphangiogenic factors and exert co-operative effect compared to siDDR1.

Note: Supplementary information is available on the Molecules and Cells website (www.molcells.org).

ACKNOWLEDGMENTS

This research was supported by the Bio & Medical Technology Development Program of the NRF, funded by the Korean government [MSIP(2015M3A9B6073827)] and by the Research Fund of Seoul St. Mary Basic Science Catholic University of Korea.

REFERENCES

Arnaoutova, I., George, J., Kleinman, H., and Benton, G. (2009). The endothelial cell tube formation assay on basement membrane turns 20: state of the science and the art. Angiogenesis *12*, 267-274.

Bachmann, B., Bock, F., Wiegand, S., Maruyama, K., Dana, M., Kruse, F., Luetjen-Drecoll, E., and Cursiefen, C. (2008). Promotion of graft survival by vascular endothelial growth factor a neutralization after high-risk corneal transplantation. Arch. Ophthalmol. *126*, 71-77.

Bartel, D.P. (2009). MicroRNAs: target recognition and regulatory functions. Cell *136*, 215-233.

Borza, C.M., and Pozzi, A. (2014). Discoidin domain receptors in disease. Matrix Biol. *34*, 185-192.

Breiteneder-Geleff, S., Soleiman, A., Kowalski, H., Horvat, R., Amann, G., Kriehuber, E., Diem, K., Weninger, W., Tschachler, E., Alitalo, K., et al. (1999). Angiosarcomas express mixed endothelial phenotypes of blood and lymphatic capillaries: podoplanin as a specific marker for lymphatic endothelium. Am. J. Pathol. *154*.

Bruick, R.K., and McKnight, S.L. (2001). A conserved family of prolyl-4-hydroxylases that modify HIF. Science *294*, 1337-1340.

Das, S., Ongusaha, P., Yang, Y., Park, J., Aaronson, S., and Lee, S. (2006). Discoidin domain receptor 1 receptor tyrosine kinase induces cyclooxygenase-2 and promotes chemoresistance through nuclear factor-kappaB pathway activation. Cancer Res. *66*, 8123-8130.

Fau, F.A., Fau, C.E., and Sathyanarayana, P. (2012). miR-199b-5p directly targets PODXL and DDR1 and decreased levels of miR-199b-5p correlate with elevated expressions of PODXL and DDR1 in acute myeloid leukemia. Am. J. Hematol. *87*, 442-446.

Flister, M., Wilber, A., Hall, K., Iwata, C., Miyazono, K., Nisato, R., Pepper, M., Zawieja, D., and Ran, S. (2010). Inflammation induces lymphangiogenesis through up-regulation of VEGFR-3 mediated by NF-kappaB and Prox1. Blood. *115*, 418-429.

Goyal, S., Chauhan, S., ElAnnan, J., Nallasamy, N., Zhang, Q., and Dana, R. (2010). Evidence of corneal lymphangiogenesis in dry eye disease: a potential link to adaptive immunity? Arch. Ophthalmol. *128*, 819-824.

Grimaldo, S., Yuen, D., Theis, J., Ng, M., Ecoiffier, T., and Chen, L. (2015). MicroRNA-184 Regulates Corneal Lymphangiogenesis. Invest. Ophthalmol. Vis. Sci. *56*, 7209-7213.

Heinzelmann-Schwarz, V., M., G.-G., Henshall, S., Scurry, J., Scolyer, R., Davies, M., Heinzelmann, M., Kalish, L., Bali, A., Kench, J., et al. (2004). Overexpression of the cell adhesion molecules DDR1, Claudin 3, and Ep-CAM in metaplastic ovarian epithelium and ovarian cancer. Clin. Cancer Res. *10*, 4427-4436.

Hu, Y., Liu, J., Jiang, B., Chen, J., Fu, Z., Bai, F., Jiang, J., and Tang, Z. (2014). MiR-199a-5p loss up-regulated DDR1 aggravated colorectal cancer by activating epithelial-to-mesenchymal transition related signaling. Dig. Dis. Sci. *59*, 2163-2172.

Jackson, D., Prevo, R., Clasper, S., and Banerji, S. (2001). LYVE-1, the lymphatic system and tumor lymphangiogenesis. Trends Immunol. *22*, 317-321.

Johansson, F., Göransson, H., and Westermark, B. (2005). Expression analysis of genes involved in brain tumor progression driven by retroviral insertional mutagenesis in mice. Oncogene *24*, 3896-3905.

Jussila, L., and Alitalo, K. (2002). Vascular growth factors and lymphangiogenesis. Physiol. Rev. *82*, 673-700.

Kerjaschki, D., Fau, B.-H.Z., Fau, R.M., Fau, S.V., Fau, S.C., Fau, W.S., Fau, B.G., Fau, K.S., Fau, K.R., Fau, H.B., et al. (2011). Lipoxygenase mediates invasion of intrametastatic lymphatic vessels and propagates lymph node metastasis of human mammary carcinoma xenografts in mouse. J. Clin. Invest. *121*, 2000-2012.

Kim, H., Choi, H., and Lee, S.K. (2015). Epstein-Barr virus miR-BART20-5p regulates cell proliferation and apoptosis by targeting BAD. Cancer Lett. *356*, 733-742.

Lam, J.K., Chow, M.Y., Zhang, Y., and Leung, S.W. (2015). siRNA Versus miRNA as therapeutics for gene silencing. Mol. Ther. Nucleic Acids *4*, e252

Leitinger, B. (2014). Discoidin domain receptor functions in physiological and pathological conditions. Int. Rev. Cell Mol. Biol. *310*, 39-87.

Leitinger, B., and Hohenester, E. (2007). Mammalian collagen receptors. Matrix Biol. *26*, 146-155.

Ling, S., Lin, H., Xiang, D., Feng, G., and Zhang, X. (2008). Clinical and experimental research of corneal lymphangiogenesis after keratoplasty. Ophthalmologica *222*, 308-316.

Ling, S., Fau, L.H., Fau, L.L., Fau, X.J., Fau, X.C., Fau, Z.W., and Liu, Z. (2009). Development of new lymphatic vessels in alkali-burned corneas. Acta Ophthalmol. *87*, 315-322.

Lossner, C., Fau, M.J., Fau, W.U., Fau, R.M., Fau, L.P., Fau, P.A., and Schnolzer, M. (2011). Quantitative proteomics identify novel miR-155 target proteins. PLoS One *6*, e22146.

Lu, Q.P., Chen, W.D., Peng, J.R., Xu, Y.D., Cai, Q., Feng, G.K., Ding, K., Zhu, X.F., and Guan, Z. (2016). Antitumor activity of 7RH, a discoidin domain receptor 1 inhibitor, alone or in combination with dasatinib exhibits antitumor effects in nasopharyngeal carcinoma cells. Oncology Lett. *12*, 3598-3608.

Mata, R., Palladino, C., Nicolosi, M.L., Presti, A.R., Malaguarnera, R., Ragusa, M., Sciortino, D., Morrione, A., Maggiolini, M., Vella, V., et al. (2016). IGF I induces upregulation of DDR1 collagen receptor in breast cancer cells by suppressing MIR-199a-5p through the PI3K/AKT pathway. Oncotarget *7*, 7683-7700.

Nakanishi, M., Morita, Y., Hata, K., and Muragaki, Y. (2016). Acidic microenvironments induce lymphangiogenesis and IL-8 production via TRPV1 activation in human lymphatic endothelial cells. Exp. Cell Res. *345*, 180-1889.

Paavonen, K., Puolakkainen, P., Jussila, L., Jahkola, T., and Alitalo, K. (2000). Vascular endothelial growth factor receptor-3 in lymphangiogenesis in wound healing. Am. J. Pathol. *156*, 1499-1504.

Regenfuss, B., Bock, F., Parthasarathy, A., and Cursiefen, C. (2008). Corneal (lymph)angiogenesis--from bedside to bench and back: a tribute to Judah Folkman. Lymphat Res. Biol. *6*, 191-201.

Sakamoto, O., Suga, M., Suda, T., and Ando, M. (2001). Expression of discoidin domain receptor 1 tyrosine kinase on the human bronchial epithelium. Eur. Respir. J. *17*, 969-974.

Seo, M., Choi, J.S., Rho, C.R., Joo, C.K., and Lee, S.K. (2015). MicroRNA miR-466 inhibits Lymphangiogenesis by targeting prospero-related homeobox 1 in the alkali burn corneal injury model. J. Biomed. Sci. *22:3*.

Shen, Q., Cicinnati, V., Zhang, X., Iacob, S., Weber, F., Sotiropoulos, G., Radtke, A., Lu, M., Paul, A., Gerken, G., et al. (2010). Role of microRNA-199a-5p and discoidin domain receptor 1 in human hepatocellular carcinoma invasion. Mol. Cancer *9*, 227.

Shrivastava, A., Radziejewski, C., Campbell, E., Kovac, L., McGlynn, M., Ryan, T., Davis, S., Goldfarb, M., Glass, D., Lemke, G., et al. (1997). An orphan receptor tyrosine kinase family whose members serve as nonintegrin collagen receptors. Mol. Cell *1*, 25-34.

Song, J., Chen, X., Bai, J., Liu, Q., Li, H., Xie, J., Jing, H., and Zheng, J. (2016). Discoidin domain receptor 1 (DDR1), a promising biomarker, induces epithelial to mesenchymal transition in renal cancer cells. Tumour Biol. *37*, 11509-11521.

Vogel, W., Gish, G., Alves, F., and Pawson, T. (1997). The discoidin domain receptor tyrosine kinases are activated by collagen. Mol. Cell. *1*, 13-23.

Wissmann, C., and Detmar, M. (2006). Pathways targeting tumor lymphangiogenesis. Clin. Cancer Res. *12*, 6865-6868.

Xiao, Q., Jiang, Y., Liu, Q., Yue, J., Liu, C., Zhao, X., Qiao, Y., Ji, H., Chen, J., and Ge, G. (2015). Minor type IV collagen alpha5 chain promotes cancer progression through discoidin domain receptor-1. PLoS Genet. *11*.

Xu, X., Fau, W.S., Fau, L.J., Fau, D.D., Fau, L.L., Fau, C.Z., Fau, Y.L., Fau, L.H., Fau, H.Q., Fau, R.J., et al. (2012). Hypoxia induces downregulation of soluble guanylyl cyclase beta1 by miR-34c-5p. J. Cell Sci. *125*, 6117-6126.

Yamanaka, R., Arao, T., Yajima, N., Tsuchiya, N., Homma, J., Tanaka, R., M., S., Oide, A., Sekijima, M., and Nishio, K. (2006). Identification of expressed genes characterizing long-term survival in malignant glioma patients. Oncogene *25*, 5994-6002.

Yang, J.F., Walia, A., Huang, Y.H., Han, K.Y., Rosenblatt, M.I., Azar, D.T., and Chang, J.H. (2016). Understanding lymphangiogenesis in knockout models, the cornea, and ocular diseases for the development of therapeutic interventions. Surv. Ophthalmol. *61*, 272-296.

Ying, S. Y., Chang, D.C., Miller, J.D., and Lin, S.L. (2006). The microRNA: overview of the RNA gene that modulates gene functions. Methods Mol. Biol. *342*, 1-18.

Zhu, J., Fau, D.-F.J., Fau, C.M., Fau, P.P., Fau, H.K., Fau, H.Y., Fau, D.M., Fau, R.M., Fau, C.J., and Azar, D.T. (2015). Simultaneous in vivo imaging of blood and lymphatic vessel growth in Prox1-GFP/Flk1::myr-mCherry mice. FEBS J. *282*, 1458-1467.